

## MICROSTRUCTURE AND MECHANICAL PROPERTIES OF AN AZ91 MAGNESIUM ALLOY PROCESSED THROUGH BACKWARD EXTRUSION

A cast AZ91 magnesium alloy was processed via backward extrusion (BE) method at different temperatures of 250, 350 and 450°C. Metallography investigations were conducted at three different regions of BE-processed cup (wall, bottom and flow channel). The main feature observed at the wall of the BE cup was mechanical twins, the frequency of which was decreased by increasing the process temperature. Flow localization in the form of shear banding occurred within the flow channel at all deformation temperatures. The bottom of the BE-processed cup at 250°C exhibited coarse initial grains along with continuous network of eutectic phase at the grain boundaries. However, increasing the process temperature to 350 and 450°C led to the fragmentation of the  $\gamma$ -Mg<sub>17</sub>Al<sub>12</sub> network down to the fine particles, where a considerable grain refinement was also traced particularly at 450°C. Furthermore, shear punch testing method was employed to evaluate the room temperature mechanical properties of the backward extruded specimens. The results show that BE-processed material would benefit from higher strength compared to the as-received material; however, the ductility follows different trends depending on the deformation temperature.

*Keywords:* magnesium alloy, extrusion, mechanical properties, shear punch test

### 1. Introduction

Generally, commercial cast magnesium alloys can be categorized in two classes; i) Mg-Al-Zn (AZ) and Mg-Al-Mn (AM) systems, developed for room temperature strength and ductility; ii) Mg-Al-RE (AE) and Mg-Al-Si (AS) systems, developed for improved elevated temperature performance [1]. In the case of AZ magnesium alloys, no reliable grain refining additive exists due to the interaction between impurity elements (such as zirconium) and aluminum, thereby resulting in poor grain refinement [1,2]. Thus, the cast AZ magnesium alloys particularly the series with high aluminum content such as AZ91 alloy, exhibit low level of strength and ductility due to very coarse grains and the presence of continuous network of eutectic phase at the grain boundaries. Therefore, in order to improve the mechanical properties of high Al-content cast AZ magnesium alloys, it is crucial to modify the morphology and distribution of  $\gamma$ -Mg<sub>17</sub>Al<sub>12</sub> phase and refine the Mg matrix grains.

It was well documented that employing various thermomechanical cycles can remarkably influenced the morphology and distribution of  $\gamma$ -Mg<sub>17</sub>Al<sub>12</sub> phase as well as grain structure [3-5]. Recent researches showed that applying severe plastic deformation using various methods, such as equal channel angular press (ECAP) [6,7], accumulative roll bonding (ARB) [8], friction stir processing (FSP) [9], and accumulative back extrusion (ABE)

[10,11] was successful in enhancing the mechanical properties of cast AZ-series magnesium alloys. However, compared to the application of repetitive working via severe plastic deformation, imposing conventional thermomechanical processing methods seems to be industrially more feasible to meet many industrial demands of superior mechanical properties at low cost and sound production performance. In this regard, quite a few studies investigated the influence of applying these conventional methods on the mechanical properties of cast AZ-series magnesium alloys [12-15]. The results showed that the employed techniques could significantly improve the ductility and strength of these alloys through modification of both  $\gamma$ -Mg<sub>17</sub>Al<sub>12</sub> phase and grains structure. It has been reported that using forward extrusion at 270°C led to a considerable grain refinement in AZ91 alloy through occurrence of dynamic recrystallization (DRX) in the presence of large number of small eutectic particles [16,17]; the associated microstructure resulted in improvement of tensile properties of AZ91 magnesium alloy. Furthermore, Kamado et al [16] studied the effects of extrusion ratio and deformation temperature on the microstructure and mechanical properties of AZ91 magnesium alloy processed via forward extrusion. The results indicated that the as-extruded alloy possesses better tensile properties compared to the cast alloy. It was reported that the average grain size became larger by increasing deformation temperature and extrusion ratio. In addition, the tensile strength

\* UNIVERSITY OF TEHRAN, THE COMPLEX LABORATORY OF HOT DEFORMATION AND THERMOMECHANICAL PROCESSING OF HIGH PERFORMANCE ENGINEERING MATERIALS, SCHOOL OF METALLURGY AND MATERIALS ENGINEERING, COLLEGE OF ENGINEERING, TEHRAN, IRAN

\*\* SCHOOL OF MECHANICAL ENGINEERING, SHAHID RAJAEI TEACHER TRAINING UNIVERSITY, TEHRAN, IRAN

# Corresponding author: m.fatemi@ut.ac.ir

increased and elongation decreased with decreasing extrusion ratio or decreasing process temperature. In spite of numerous conducted researches, proposing suitable thermomechanical processing routes to introduce microstructural refinement in the cast high aluminum AZ-Mg ingots is still an appealing challenge to overcome their limited strength and ductility.

Among the different conventional deformation processing methods, the backward extrusion (BE) has become one of the most promising manufacturing processes which can produce precise near-net-shape parts [18]. Nevertheless, the most published researches in this regard have been focused on the aluminum alloys. For instance, the BE process has been applied on the 7075 aluminum alloy and the results showed that the process can refine the grains and improve the subsequent mechanical properties of the experimental alloy [19]. However, in the case of cast magnesium alloys there is no systematic investigation on microstructure evolution and subsequent mechanical properties developed during BE process. Therefore, the aim of this study has been directed toward the investigation of microstructure evolution of cast AZ91 magnesium alloy considering the effects of process temperature. Moreover, the mechanical properties of BE-products processed at various temperatures have been evaluated using Microhardness as well as shear punch testing methods.

## 2. Experimental section

### 2.1. Material and process

The experimental AZ91 alloy was received in as-cast condition with the chemical composition of Mg-9.04Al-1.09Zn-0.21Mn (wt. %). As is shown in Figure 1, the initial microstructure is composed of three different phases, namely primary  $\alpha$ -Mg phase, the  $\gamma$ -precipitates ( $Mg_{17}Al_{12}$ ) and the eutectic phase ( $\alpha+\gamma$ ). The grain size of the initial structure was measured to be about 300  $\mu m$ . The BE process was carried out on the cylindrical workpieces in the sizes of  $\Phi 18 \times 8$  mm (Fig. 2a). To minimize the friction during the process,  $MoS_2$  lubricant was pasted to the surface of the workpieces and dies. A punch diameter of 12 mm was selected and this yields a cup shape product of 3 mm wall thickness. The die was heated up to the process temperature by using a jacket furnace. The workpieces were heated to the predetermined temperatures in a resistant furnace and held for 10 min to equation the temperature. Finally, the workpieces were back extruded at temperatures of 250, 350, and 450°C using a computerized universal testing machine at a constant ram speed of 5 mm/min. All the BE tests were performed through penetrating the punch by depth of 6 mm into the specimen. The

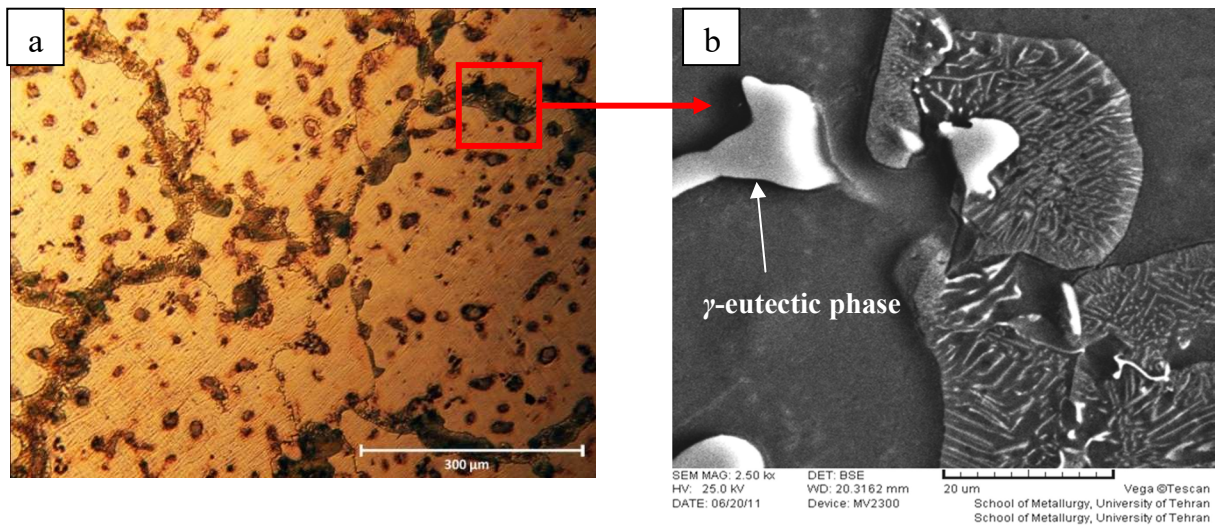


Fig. 1. The typical microstructures of the as-cast AZ91 alloy (a) optical microstructure, (b) SEM image

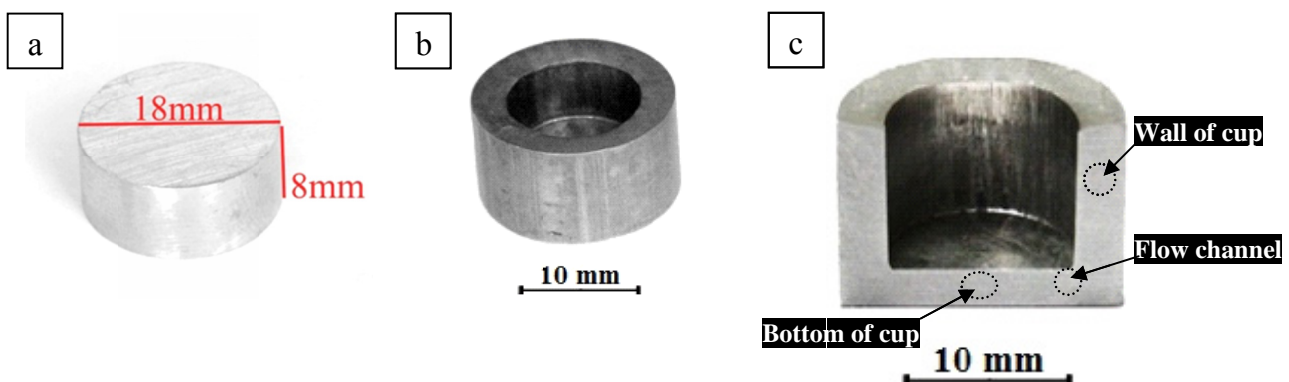


Fig. 2. (a) The BE workpiece before processing, (b) after processing (c) the cross section of BE-processed spec

BE processing has been successfully carried out with no danger of crack or discontinuity. After deformation, to preserve the obtained microstructure, the processed specimens were immediately quenched into water. The typical BE-processed specimen is shown in Figure 2b. In order to examine microstructure, the processed workpieces were cut parallel to the extrusion direction (Fig. 2c). The obtained cross section was mechanically polished and etched for 7 s using a solution of 70 ml ethanol, 4.2 g picric acid, 10 ml acetic acid and 10 ml water. The obtained microstructures were examined by a MEIJI optical microscope (OM).

## 2.2. Mechanical Testing

### 2.2.1. Shear punch testing method

The small specimen shear punch testing (SPT) method [20] was employed to evaluate the room temperature mechanical properties of the processed and as-received materials. Back extruded specimens were sliced to the approximate thickness of 800  $\mu\text{m}$  employing wire cutting method. The SPT specimens were extracted from the bottom region of the cups as it is indicated in Figure 2c. In order to remove the oxidation and surface melting imperfection which might be formed due to the cutting process, any specimen surface was mechanically polished to a final thickness of  $600 \pm 15 \mu\text{m}$  and located in specially designed fixture with a  $1.5 \pm 0.005 \text{ mm}$  diameter flat cylindrical punch and  $1.54 \pm 0.005 \text{ mm}$  diameter receiving-hole. Finally, minimum three shear punch tests were carried out on each slice at the room temperature using an Instron 4208 machine with constant cross-head speed of 0.2 mm/min. The load-displacement data was converted to shear stress-displacement data using equation (1).

$$\tau = \frac{P - F}{2\pi r t} \quad (1)$$

Where  $P$  is the applied load,  $F$  is the friction load,  $t$  is the specimen thickness,  $r$  is the average of punch and receiving-hole radii. The related data acquisition and result analyses have been thoroughly explained elsewhere[14].

### 2.2.2. Hardness

Micro-hardness testing was carried out using a load of 20 gram with 15 s dual time to investigate the effect of flow localization on microhardness of material at different BE temperatures.

## 3. Result and discussions

### 3.1. Load-Displacement diagrams

The punch load versus punch displacement curves during BE process at different deformation temperatures are presented

in Figure 3. As is seen, the punch load level is significantly affected by deformation temperature. The load levels monitored during BE at 350 and 450°C have been smoothly decreased from displacements of about 2.5 and 2 mm, respectively. On the contrary, no dynamic load lessening is seen during BE at 250°C. The latter load level reduction could be attributed to the activation of restoration mechanisms (i.e. dynamic recovery and recrystallization) at high deformation temperatures.

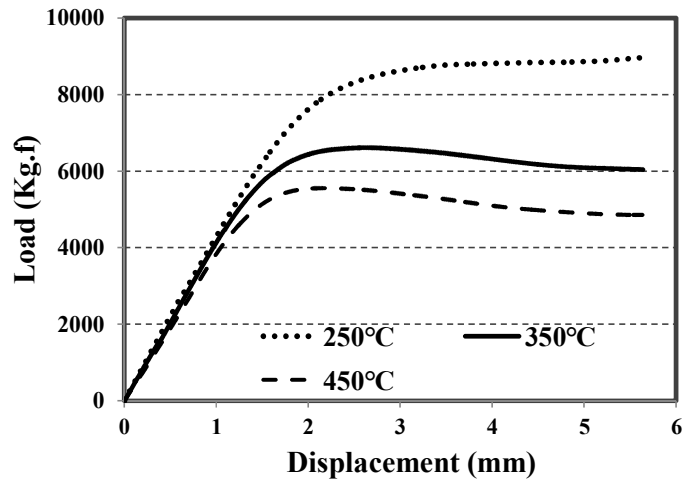


Fig. 3. Punch Load-Displacement obtained from BE process at different temperatures

### 3.2. Microstructure evolution

Since the backward extrusion is a near net shape process, the processed material is almost directly used as an ultimate operating part of a system. As a result, its microstructure and corresponding mechanical properties of processed workpiece across whole cross section are of high importance affecting its performance during application lifecycle. In this regard, Fatemi et al. [21]. Investigated the development of equation plastic strain (EPS) and shear strain (SS) during BE process of AZ91 magnesium alloy. The obtained results showed that the distribution of EPS and SS followed a heterogeneous pattern. In other words, different values of EPS and SS are imposed to the different regions of the processed workpiece. Therefore, in order to trace the effect of deformation temperature on the microstructure evolution of processed material at different regions, three main areas including wall, bottom and flow channel of the BE cup have been chosen (see Fig. 2c). In the following sections, the effect of deformation temperature of 250, 350 and 450°C on the microstructure characteristics of each three regions will be discussed in details.

#### 3.2.1. Wall of cup

The microstructures obtained at the wall of the BE cup at different temperatures have been shown in Figure 4. As is depicted, twinning has significant contribution to the accommodation of imposed strain at all deformation temperatures,

even at high temperature of 450°C. It can be attributed to the large grain size of initial cast experimental alloy which promotes the formation of twins during deformation; additionally, strain complexity imposed during BE may promote the occurrence of the twinning even at high BE temperatures. However, it is obvious that as the temperature decreased from 450°C to 250°C, the frequency of twinning (i.e. number of twins per unit area) drastically increased. As is well known, the critical resolved shear stress (CRSS) for non-basal slip systems remarkably

increase with decrease of deformation temperature; therefore, the imposed strain is mostly accommodated by twinning. More precise investigations into the microstructure of wall of the BE cup using higher magnification revealed that no new DRX grains have been detected at lower deformation temperatures of 250 and 350°C (Fig. 4d,e). On the other hand, as is seen in Figure 4f, very fine DRX grains are formed within the mechanical twins through twin DRX mechanism which was already reported during hot deformation of AZ-Mg alloys [3,17].

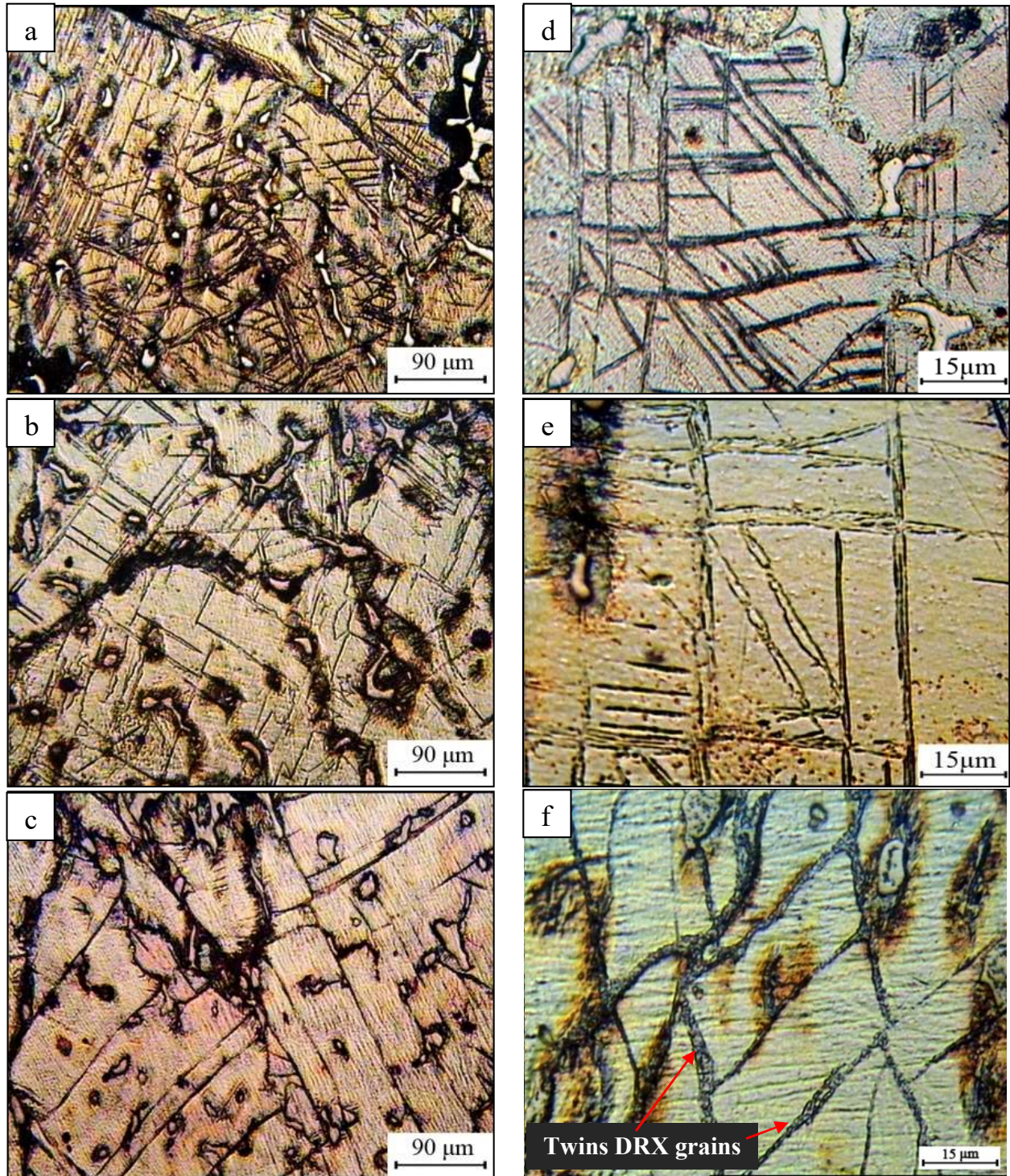


Fig. 4. The microstructures developed at the wall region of the specimens backward extruded at (a) and (d) 250°C, (b) and (e) 350°C, (c) and (f) 450°C

### 3.2.2. Flow channel

During backward extrusion, due to geometry of process, deformation is progressively introduced through the flow channel (see Fig. 2c) within which a high magnitude of shear strain is imposed [21]. Figure 5 shows the microstructures of the flow channel at various deformation temperatures. Distinguishable narrow regions of localized flow have been developed in the form of shear bands at all deformation temperatures. As depicted

in Figure 5, the shear bands took place more extensively at lower deformation temperatures, mainly attributed to restricted operation of activated slip systems. Optical microscopy of the shear bands at higher magnification (Fig. 5d-f) shows that at lower deformation temperatures the initial grains as well as  $\gamma$ -eutectic phases severely elongated along the shear direction (Fig. 5d). However, some elongated grains have been replaced by new fine dynamically recrystallized grains at higher temperature of 350°C (Fig. 5e). This is more pronounced at

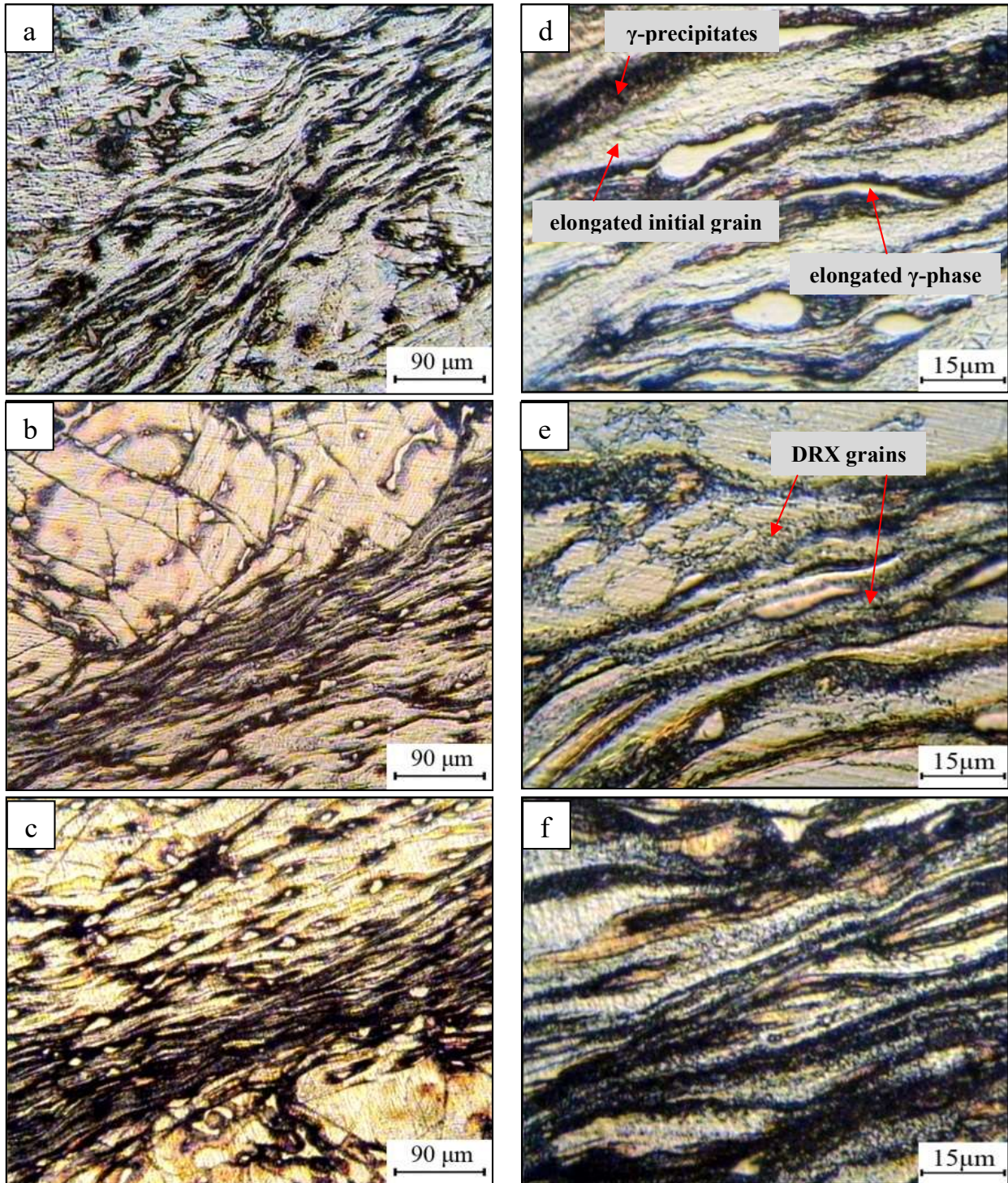


Fig. 5. The microstructures developed at the flow channel region of the specimens backward extruded at (a) and (d) 250°C, (b) and (e) 350°C, (c) and (f) 450°C

450°C (Fig. 5f), where an increase in fraction of DRX grains is observed.

When the material undergoes flow localization, the homogeneity within the specimen can be evaluated by taking microhardness measurements. This was carried out at regions of shear band interior and exterior. The microhardness results are indicated in Figure 6. Higher microhardness values were recorded inside the shear bands. This may be related at 250°C to the high dislocation density and at 350 and 450°C to the significant grain refinement inside the bands (see Fig. 5). However, hardness difference between shear band interior and exterior tends to reduce with increasing BE temperature. This is rationalized considering extensive occurrence of dynamic recovery and recrystallization at higher temperature resulting improved hardness homogeneity.

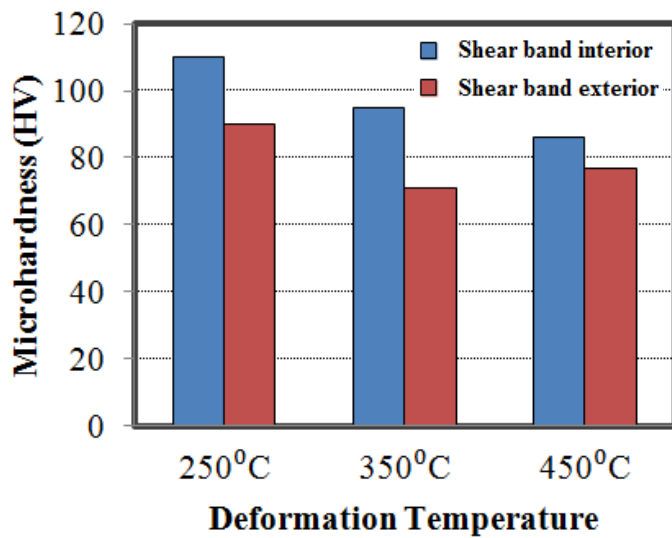


Fig. 6. The microhardness values measured inside and outside the shear bands

### 3.2.3. Bottom of cup

Figure 7 depicted the microstructure of AZ91 magnesium alloy developed at the bottom of the BE cup at the temperatures of 250, 350 and 450°C. As is seen in Figure 7a, at the deformation temperature of 250°C, the microstructure includes the coarse initial grains of cast material accompanied by continuous network of  $\gamma$ -eutectic phase at the grain boundaries. Microstructure at higher magnification (Fig. 7d) shows that mechanical twins contribute to accommodate the imposed strain; however, no DRX grains can be traced in this BE temperature. On the contrary, at higher temperatures of 350 and 450°C the continuous network of  $\gamma$ -eutectic phase fragmented into the fine particles well-distributed in the microstructure (Fig. 7b,c). Figure 8 depicts the fine eutectic phase particles crushed through BE process at 450°C. This may be facilitated at higher temperature due to lower strength of eutectic phase [22]. As is shown in Figure 7e, BE at 350°C resulted in formation of very fine grains at the vicinity of initial grain boundaries. The DRX grains volume fraction at this temperature has been measured to be about 24%. By increasing

the deformation temperature from 350 to 450°C a remarkable progress of DRX process from grain boundaries toward the interior of grains is observed (Fig. 7f), where a DRX volume fraction of 42% has been reached.

## 4. Mechanical properties

The variation of yield shear strength (YSS), ultimate shear strength (USS) and shear elongation (SE) of BE-processed samples measured through SPTs are presented in Figure 9. For the sake of comparison, the mechanical properties of as-received cast AZ91 magnesium alloy are included as well. As is clearly seen, the mechanical properties of experimental alloy are influenced by the deformation temperature. The variations of mechanical properties are justified relying on the microstructure characteristics obtained at each processing temperature.

In the case of YSS and USS, BE process at all temperatures led to increase in strength compared to the as-received material. In fact, two mechanisms may contribute to strengthening during such large deformation as backward extrusion. First, the mechanism of dislocation strengthening due to presence of incidental dislocation boundaries of small misorientation; these boundaries arise from the trapping of dislocations. The second mechanism is the conventional grain boundary strengthening via Hall-Petch effect. The proposed strengthening equation for this model containing both mechanisms may be expressed as [23]:

$$\sigma = \sigma_0 + M\alpha Gb\sqrt{\rho} + \frac{k}{\sqrt{d}} \quad (2)$$

Where  $s$  is the yield stress,  $M$  is the Taylor factor,  $\sigma_0$  the friction stress,  $\rho$  is the dislocation density,  $\alpha$  is a constant,  $d$  is the average grain or cell size and  $k$  is the Hall-Petch constant. This equation can be qualitatively taken into account to justify the variation of strength (YSS and USS) depicted in Figure 9a,b.

In the case of deformation temperature of 250°C, YSS and USS of the BE-processed specimens are higher than as-received material. This is related to the significant mechanical twins developed in the microstructure (Fig. 7a,d). Twin boundaries can act as high angle boundaries with similar Hall-Petch effect resulting in higher YSS. Due to the lack of DRX a high density of dislocation may be also anticipated in this condition. This may additionally increase the flow stress i.e. YSS and USS.

In the case of BE temperature of 350 and 450°C, the higher YSS and UTS compared to the as received material can be mainly attributed to the grain refinement occurred via DRX resulting significant lower average grain size (Fig. 7b,c). However, the strengthening is lowered in these higher temperatures compared to 250°C. This may be explained considering the promotion of restoration mechanisms, which led to effective dislocation annihilation and releasing the strain stored energy of the material.

The SE values of the BE-processed specimens as well as as-received material are shown in Figure 9c. The SE value of the as-received AZ91 was relatively low due to presence of con-

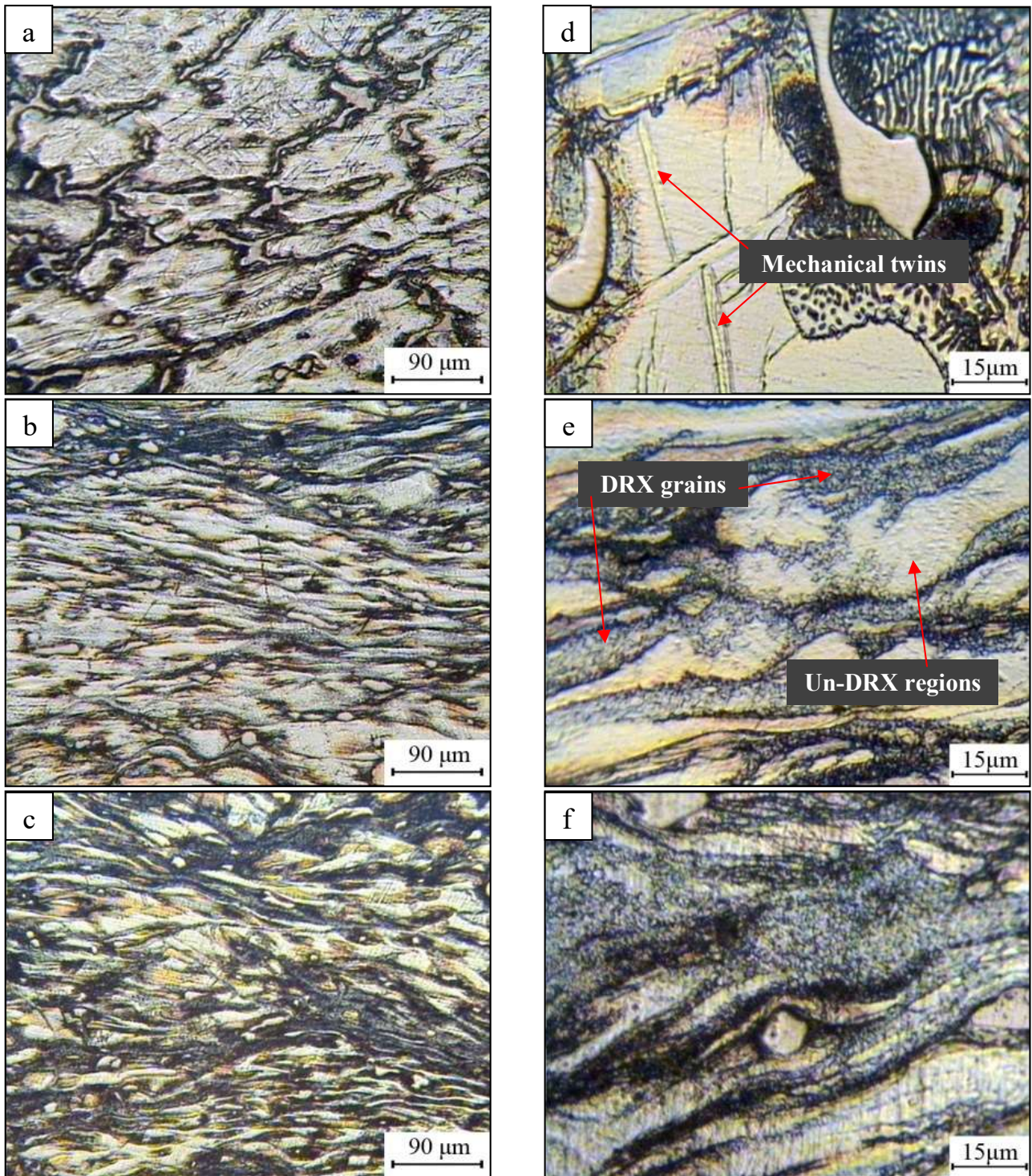


Fig. 7. The microstructures developed at the bottom region of the specimens backward extruded at (a) and (d) 250°C, (b) and (e) 350°C, (c) and (f) 450°C

tinuous network of  $\gamma$ -eutectic phase along the grain boundaries of the initial coarse grained microstructure (Fig. 1). Ding et al. [16] have already reported the detrimental effect of the massive eutectic phase ( $\gamma$ ) on the elongation to fracture of AZ91 processed by ECAP; the results indicated that the cracks initiate and propagate through the  $\alpha$ -Mg/ $\gamma$  phase interface. However, the lowest SE was obtained for the BE-processed specimen at 250°C which is attributed to the high dislocation density. The latter exhausts the material's capacity for further work hardenability. Moreover,

the presence of brittle network of  $\gamma$ -eutectic phase at the grain boundaries (Figure 7a) may mitigate the ductility. On the other hand, at higher deformation temperatures of 350 and 450°C the SE increased significantly due to the occurrence of DRX and reduction in average grain size. In addition, the crushing of  $\gamma$ -eutectic phase network to the fine particles and distribution of the particles in microstructure at high temperatures may assist in the ductility enhancement. Similar effects were also reported during FSP of AZ80 magnesium alloy [1].

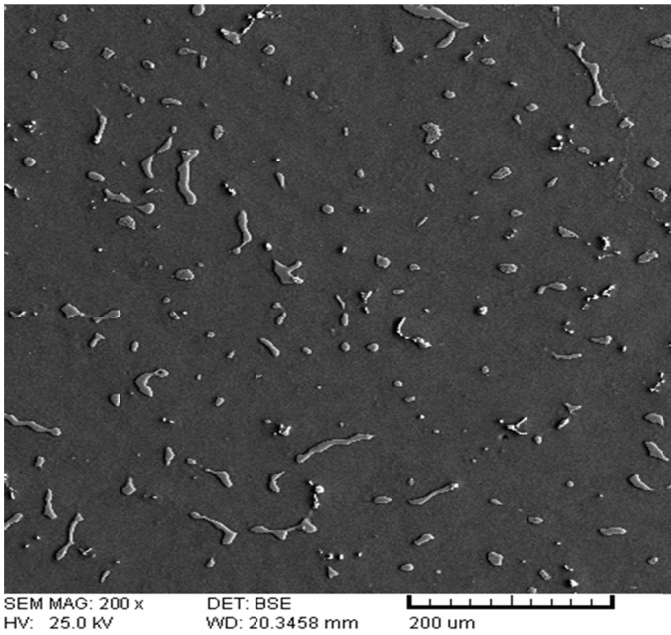


Fig. 8. The SEM micrograph of fine fragmented  $\gamma$ -eutectic phase particles in the BE-processed specimen at 450°C

In order to estimate the optimum thermomechanical condition for BE processing, the formability index parameter has been

used. The material formability can be assessed through employing USS and SE values, according to equation [3]:

$$\text{Formability Index [MPa\%]} = \text{USS [MPa]} \times \text{SE [\%]} \quad (3)$$

Figure 10 indicates the variation of formability index for different thermomechanical processing. As is observed, the formability index of all backward extruded specimens is superior to as-received material, and it has been improved with increasing the deformation temperature. It is noticeable that even though SE of the deformed specimen at 250°C is less than as-received specimen, its higher USS outweighed its low SE which led to obtaining higher formability index at 250°C compared to as-received material. As is clear in Figure 10, the highest formability index has been achieved for thermomechanical processing at 450°C, which can be introduced as an optimum condition for BE processing of cast AZ91 magnesium alloy.

### 5. Conclusion

The present study has focused on the microstructural evolution and mechanical properties of cast AZ91 magnesium alloy processed by backward extrusion at temperatures of 250,

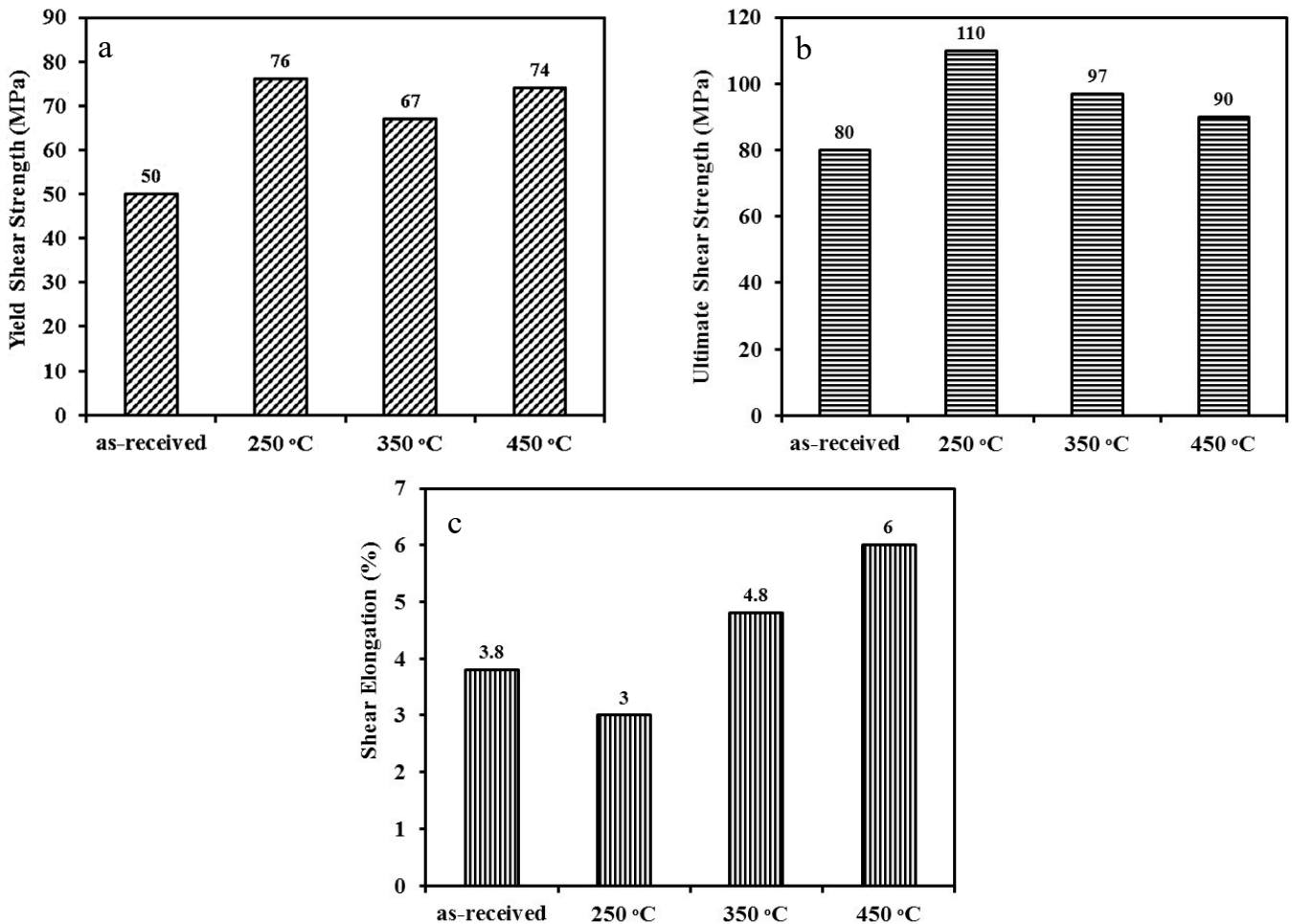


Fig. 9. The shear punch test results of processed and as-received AZ91 magnesium alloy: (a) yield shear strength (b) ultimate shear strength (c) shear elongation



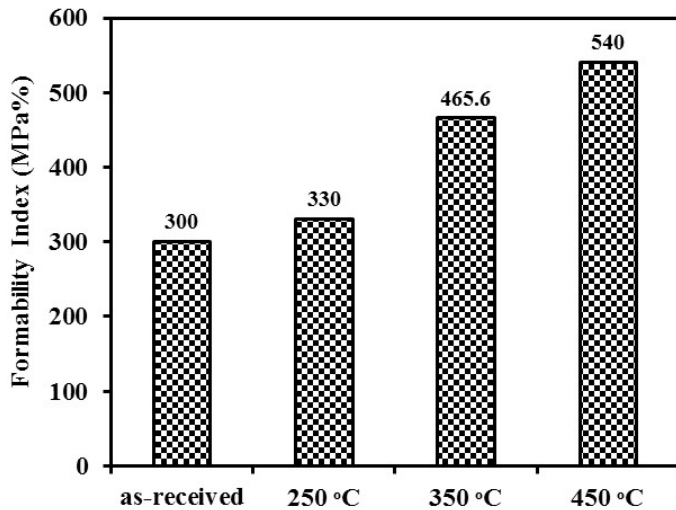


Fig. 10. The formability index of BE processed and as-received AZ91 magnesium alloy

350 and 450°C. The main points resulted from this work can be summarized as follows:

- Mechanical twins are the main feature detected in all deformation temperatures at the wall of the BE cup, where the twinning frequency was reduced by increasing the deformation temperature.
- Considerable flow localization in the form of shear banding was the main microstructure characteristic at the flow channel of BE-processed specimen cross section. Although no new DRX grains was found in the shear banding at 250°C, significant grain refinement occurred at the flow channel during BE process at 350 and 450°C.
- The coarse grains accompanied by continuous network of  $\gamma$ -eutectic phases at the grain boundaries were detected in the bottom of the BE cup at 250°C. However, increasing the process temperature to the 350 and 450°C led to fragmentation of  $\gamma$ -eutectic phases to the fine particles as well as remarkable grain refinement via DRX process.
- SPT results implied that YSS and USS were improved after BE process. The latter was attributed to the Hall-Petch effect of mechanical twins and high dislocation density at 250°C, and to significant grain refinement at 350 and 450°C.
- The variation in shear elongation showed different trends for various deformation temperatures. The decrease of SE related to the BE processing at 250°C was due to dislocation accumulation resulted in high density of dislocations; nonetheless, the increment of SE related to the BE processing at 350 and 450°C was because of DRX proceeding and considerable decrease of average grain size.

## REFERENCES

- [1] A. Feng, B. Xiao, Z. Ma, R. Chen, *Metallurgical and Materials Transactions A* **40**, 2447-2456 (2009).
- [2] M. Moradjoy-Hamedani, A. Zarei-Hanzaki, S.M. Fatemi, S. Asqardoust, *Advanced Engineering Materials*, n/a-n/a (2015).
- [3] P. Changizian, A. Zarei-Hanzaki, H. Abedi, *Materials Science and Engineering A* **558**, 44-51 (2012).
- [4] M. Maghsoudi, A. Zarei-Hanzaki, H. Abedi, A. Shamsolhodaei, *Philosophical Magazine* **95**, 3497-3523 (2015).
- [5] A. Stefanik, P. Szota, S. Mróz, T. Bajor, H. Dyja, *Archives of Metallurgy and Materials* **60**, 3001-3006 (2015).
- [6] J. Gubicza, K. Máthis, Z. Hegedűs, G. Ribárik, A.L. Tóth, *Journal of Alloys and Compounds* **492**, 166-172 (2010).
- [7] K. Máthis, J. Gubicza, N. Nam, *Journal of Alloys and Compounds* **394**, 194-199 (2005).
- [8] M.T. Pérez-Prado, J. Del Valle, O.A. Ruano, *Materials letters* **59**, 3299-3303 (2005).
- [9] A. Feng, Z. Ma, *Acta Materialia* **57**, 4248-4260 (2009).
- [10] P. Changizian, A. Zarei-Hanzaki, M. Ghambari, A. Imandoust, *Materials Science and Engineering: A* **582**, 8-14 (2013).
- [11] S. Fatemi-Varzaneh, A. Zarei-Hanzaki, *Materials Science and Engineering: A* **528**, 1334-1339 (2011).
- [12] P. Changizian, A. Zarei-Hanzaki, A.A. Roostaei, *Materials & Design* **39**, 384-389 (2012).
- [13] J. Del Valle, M.T. Pérez-Prado, O. Ruano, *Materials Science and Engineering: A* **355**, 68-78 (2003).
- [14] S. Fatemi-Varzaneh, A. Zarei-Hanzaki, H. Beladi, *Materials Science and Engineering: A* **456**, 52-57 (2007).
- [15] K. Hirai, H. Somekawa, Y. Takigawa, K. Higashi, *Materials Science and Engineering: A* **403**, 276-280 (2005).
- [16] H. Ding, L. Liu, S. Kamado, W. Ding, Y. Kojima, *Journal of alloys and compounds* **456**, 400-406 (2008).
- [17] S. Xu, S. Kamado, N. Matsumoto, T. Honma, Y. Kojima, *Materials Science and Engineering: A* **527**, 52-60 (2009).
- [18] D. Hinz, A. Kirchner, D. Brown, B.-M. Ma, O. Gutfleisch, *Journal of materials processing technology* **135**, 358-365 (2003).
- [19] M. Rokni, A. Zarei-Hanzaki, H. Abedi, *Materials Science and Engineering: A* **532**, 593-600 (2012).
- [20] R. Guduru, R. Scattergood, C. Koch, K. Murty, A. Nagasekhar, *Metallurgical and Materials Transactions A* **37**, 1477-1483 (2006).
- [21] A. Chalay-Amoly, A. Zarei-Hanzaki, P. Changizian, S. Fatemi-Varzaneh, M. Maghsoudi, *Materials & Design* **47**, 820-827 (2013).
- [22] Z. Zhao, Q. Chen, C. Hu, S. Huang, Y. Wang, *Journal of Alloys and Compounds* **485**, 627-636 (2009).
- [23] G.E. Dieter, D. Bacon, *Mechanical metallurgy*, McGraw-Hill New York, 1986.